



PERGAMON

Available online at www.sciencedirect.com

SCIENCE @ DIRECT®

Electrochimica Acta 48 (2003) 3599–3605

ELECTROCHIMICA
Acta

www.elsevier.com/locate/electacta

The electrochemical behavior of tin-doped indium oxide during reduction in 0.3 M hydrochloric acid

C.A. Huang^{a,*}, K.C. Li^a, G.C. Tu^b, W.S. Wang^b

^a Department of Mechanical Engineering, Chang-Gung University, Taoyuan, Taiwan 333, China

^b Department of Materials Science and Engineering, Chiao-Tung University, Hsinchu, Taiwan, China

Received 10 March 2003; received in revised form 2 June 2003; accepted 5 June 2003

Abstract

The electrochemical behavior of tin-doped indium oxide (ITO) on SiO₂ in 0.3 M HCl was studied using voltammetric scanning method. The result showed that an obvious reduction current peak occurred during the first cathodic potential scanning. The reduction reaction became less active after annealing ITO at 500 °C for 1 h. The result was attributed to the replenishment of oxygen-deficient site, which acts as current carrier, by the annealing treatment. Many spherical In–Sn particles with sizes about 100–500 nm were formed on the ITO surface adjacent to the grain boundary when the reduction current took place. The In–Sn particles initiated preferentially on the ITO surface near grain boundaries attending the dissolution of ITO grain boundary. In the scanning period, after completion of the reduction current peak, reduction of hydrogen ions occurred in more negative potential region. A schematic illustration for the formation mechanism of the In–Sn reduction particle was postulated based on the metallographical and electrochemical results in this work.

© 2003 Elsevier Ltd. All rights reserved.

Keywords: Tin-doped indium oxide; Voltammetric scanning; Reduction product; In–Sn particle; FESEM; EDS

1. Introduction

Tin-doped indium oxide (ITO) is an oxide film composed of mainly In₂O₃ with ca. 10 wt.% SnO₂. ITO, which has its high optical transmittance (more than 80–90% at 550 nm wavelength) and low sheet resistivity (lower than $2 \times 10^{-4} \Omega \text{ cm}$), is an important optoelectronic material. Popular applications of ITO are found in electronic and photoelectric devices, such as the electrical conducting element, liquid crystal display (LCD), light-emitted diode (LED) and organic electroluminescent display (OLED) [1–4]. The donors of ITO are contributed principally from the oxygen vacancies and the substitutional tin-dopants formed in the lattice of indium oxide during the growing process [5].

The electronic and structural properties [6] as well as the electrochemical behavior of the ITO have been investigated for some time. Bruneaux et al. [7] pointed

out that very slow transfer kinetics for the oxide was affected by the redox potential and the chemical species in the solution. In addition, Bressers and Meulenkamp [8] studied the ITO electrodes in propylene carbonate solutions containing lithium ions by using X-ray diffraction, ultraviolet–visible and quartz crystal microbalance. From their results, the cathodic reaction involved the reduction of electrolyte at $E \geq 1.0 \text{ V vs. Li/Li}^+$, and led to the formation of a thin lithium-rich film.

Various interesting results on the study of electrochemical behavior of ITO in HCl solution have also been reported [9,10]. Among them, Folcher et al. [9] proposed the two-step anodic dissolution mechanism of ITO in 0.04 and 0.1 M HCl solutions. In the theory, they assert that radical species, OH• and Cl•, are first generated by electrochemical reaction, and then In–O bonds on the surface are broken by the radical species. In addition, Bard et al. [10] had studied the relationship between the mixed potential and dissolution rate of ITO. They have confirmed that the anodic dissolution

* Corresponding author. Tel.: +886-3-211-8800x5346; fax: +886-3-397-3340.

E-mail address: gfehu@mail.cgu.edu.tw (C.A. Huang).

potential of the ITO is located closely at the redox potential of Cl^-/Cl_2 reaction (ca. 1.15 V vs. SCE).

In general, voltammetric scanning (VS) is a useful electrochemical method to monitor the species reaction in electrolyte. In particular, the phenomenon of the complex redox reaction of ITO can be explained by the result derived from VS measurement. For example, Monk and Man [11] had studied the dissolution behavior of ITO in acidic solution through VS measurement. The equation of the reaction, $\text{ITO} + x(\text{M}^+ + \text{e}^-) \rightarrow \text{M}_x\text{ITO}$, yields a hydro-film, which was obtained through applying the negative potential to the ITO. It would obstruct the migration rate of the carrier in ITO. Besides, Wang and Hu [12] investigated the structural and electrochemical characterization of ‘open-structured’ ITO using VS test. The open-structured ITO was deposited by RF-diode sputtering and their VS results showed that the ITO has the considerable reversible charging capacity in 1 M LiClO_4 /propylene carbonate solution. Although some reaction mechanisms of ITO in various electrolytes using VS method were proposed, little is known about the microstructure variation of ITO after VS test in hydrochloric acid. This issue will be addressed in this research.

The VS behaviors of the as-received, 200 and 500 °C annealed ITO in 0.3 M HCl were studied. In particular, the reaction products of ITO after VS experiment were examined and analyzed with field-emission scanning electron microscope (FESEM) integrated with energy-dispersive X-ray spectrometer analysis (EDS) for chemical compositional analysis. The correlation between the VS behavior of the ITO and their microstructure was established. A new dissolution mechanism of ITO in 0.3 M HCl was proposed.

2. Experimental

The ITO was deposited on the glass substrate by sputtering and a buffer layer of SiO_2 was sandwiched between ITO and glass. Fig. 1 shows the TEM micrograph of as-received ITO, SiO_2 and glass in cross-sectional view [13]. The thickness of ITO, SiO_2 buffer and glass substrate were 150 nm, 20 nm, and 700 μm , respectively. The as-received ITO was prepared from a SUMITOMO DC-diode sputtering system, and the source target composed of 90 wt.% In_2O_3 and 10 wt.% SnO_2 . After sputtering the ITO was ozone-treated to increase its electrical conductivity. To investigate the effect of annealing temperature on the ITO, the as-received specimens were annealed in the air furnace at 200 and 500 °C for 1 h. Subsequently, the ITO specimens were ultrasonically cleaned in an acetone bath, dried with cold air before they were ready for electrochemical test and FESEM examination.

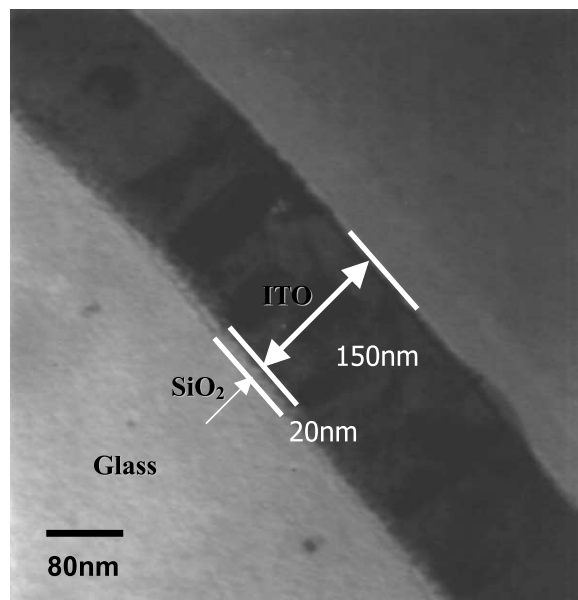


Fig. 1. TEM micrograph of the cross-sectional ITO and SiO_2 films and glass substrate.

Electrochemical measurement was performed with a Potentiostat/Galvanostat (EG&G Model 273A) and a flat cell (EG&G Model K0235). The schematic construction of the electrochemical cell used in this study is shown in Fig. 2. A platinum wire and Ag/AgCl (sat.) were used as counter and reference electrodes, respectively. The ITO, with an exposing area of 1 cm^2 , was set as the working electrode. A thin copper foil ca. 35 μm thick in a ring shape was used to connect the ITO to the testing apparatus. The electrolyte used was 0.3 M HCl. The electrochemical cell was set in a water-circulated bath to keep a constant temperature of 20 ± 0.5 °C. Nitrogen gas was purged into the electrolyte during experiment. Before VS experiment, the ITO electrode was immersed in the electrolyte for 15 min until dynamic stable was established between electrode and electrolyte.

The surface morphology of ITO after annealing and electrochemical test was examined with an FESEM (Hitachi Model S-4700) integrated with an EDS

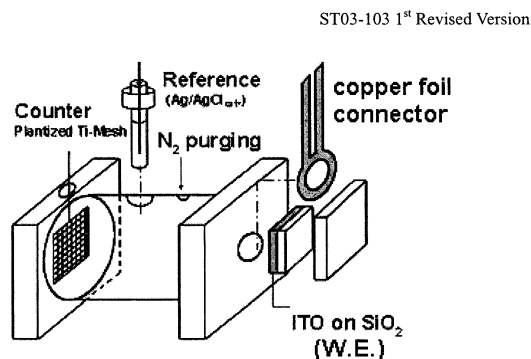


Fig. 2. Schematic construction of the electrochemical cell used in this study.

(EDAX company, series No. 8318-46390 ME). Before FESEM examination, 1–2 nm thick Pt was sputtered to the specimen surface to improve its electrical conductivity and enhance the signal of secondary electron.

3. Results and discussion

3.1. Microstructure

The FESEM micrographs of as-received and 500 °C annealed ITO are shown in Fig. 3(a). Equiaxed grains on both ITO could be seen. The grain sizes of both specimens remained virtually unchanged and were estimated to be ca. 150 nm. No significant grain growth of the ITO had occurred, although the ITO had annealed at 500 °C for 1 h. However, it has been reported that lower carrier concentration and higher resistivity of the ITO could be induced owing to decrease of oxygen deficiency in its lattice after annealing at 500 °C in the air [14,15]. The effect of annealing temperatures on the electrochemical behavior of the ITO will be further discussed in the following section.

3.2. VS studies

Fig. 4 shows the VS result of as-received ITO performed from +1.5 to –1.5 V. An obvious reduction current peak can be found in the first negative potential scanning and the peak of the reduction current is almost unobservable in the succeeding cyclic scanning. It is significant to note the presence of numerous spherical particles occurred on the surface of ITO and at the same time the grain boundaries of the ITO were dissolved after first negative potential scanning (Figs. 5(a) and (b)). This seems to suggest that the cathodic current assists depletion of the grain boundaries of the ITO and then leads to formation of the spherical particles. Figs. 5(c) and (d) show the results of EDS analyses performed for the spherical particle and the ITO substrate, A and B indicated, respectively, in Fig. 5(b). For the result of EDS analyses of the particle, elements O, Si, In and Sn

were detected, while the same elements with much weaker In and Sn signal intensities were detected for the substrate. Since the escaped depth of characteristic X-ray could be a few micrometers from the surface into the specimen by applying 5 keV electron beam, the detected elements, Si and O, would be attributed possibly to the glass substrate and SiO₂ buffer layer. Because formation of the spherical particle relates intimately with cathodic current applied and the elements, O and Si, contained in the particle are generally not a norm, thus we will resort to another experiment to rationalize this result in the next paragraph.

In order to study the effect of the cathodic current on ITO, a constant cathodic of –1.5 V was applied on ITO for 0.25 s, a very small current density, ca. 5 mA/cm², responded in this very short period. Fig. 6(a) shows the surface morphology of the ITO after this short period test. As expected, many spherical particles of size about 100–800 nm could be observed on the ITO surface and the dissolution site occurred preferentially in the grain boundaries of the ITO. Interestingly, only small amount of the reduction charge (ca. 1.25×10^{-3} C) in this experiment was enough to cause serious depletion of the grain boundaries. It is evident that the ITO, especially the grain boundaries of the ITO, was very sensitive to the cathodic potential applied.

After the short period cathodic potential applying at –1.5 V, some isolated spherical particles were directly extracted using a carbon bond; this enables composition being analyzed without interference from the characteristic X-ray signals coming from retained ITO, SiO₂ and substrate. Fig. 6(b) shows the micrograph of an isolated particle and the result of EDS analyses of local points within the particle with a 4 nm electron beam. Unlike the results of EDS analyses shown in Figs. 5(c) and (d), only In and Sn were detected within the isolated spherical particle. The chemical composition of the particle composed uniformly major of In with minor of Sn. Based on the above results, it can be recognized that the spherical particle would be derived from reduction of cations, In³⁺ and Sn²⁺, on the ITO; moreover, these cations were released mainly from the

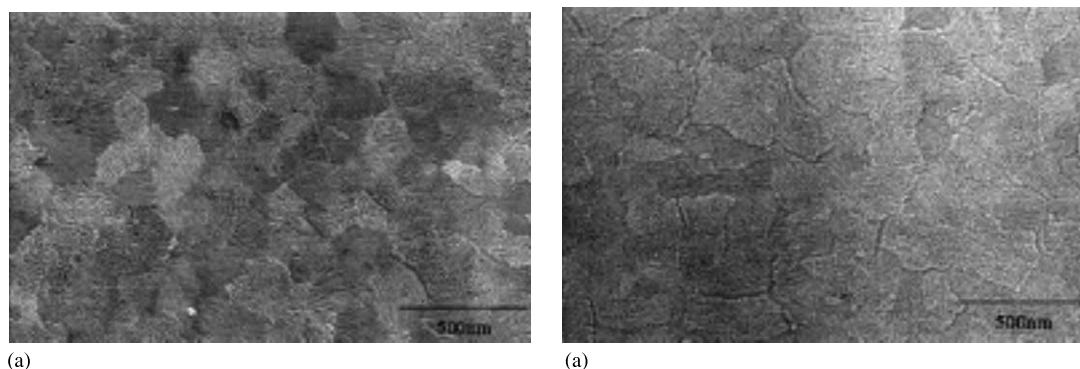


Fig. 3. The grain morphologies of (a) as-received ITO and (b) ITO after annealing at 500 °C for 1 h (FESEM).

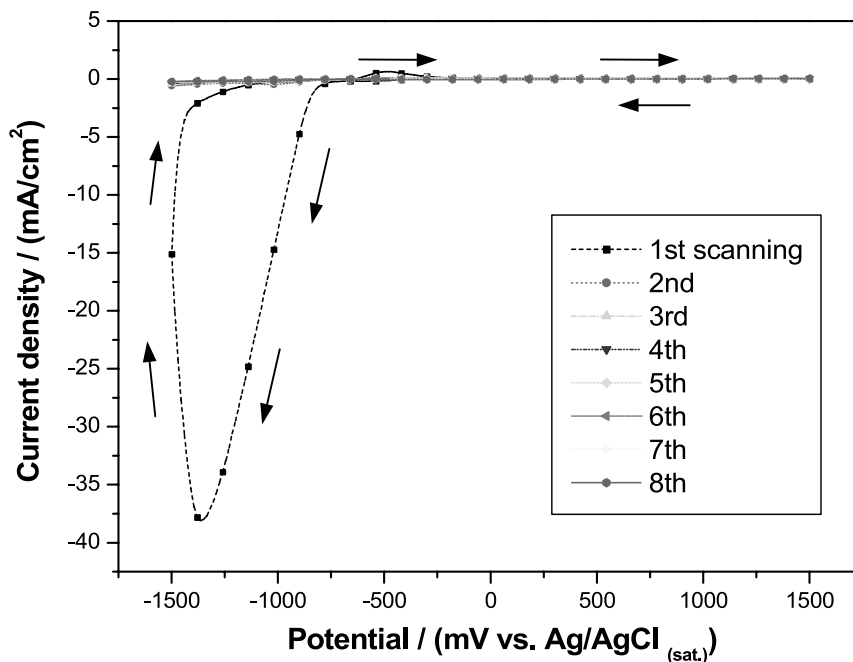


Fig. 4. The VS response of as-received ITO in 0.3 M HCl, an obvious reduction current peak obtained only in first VS scanning (scanning rate: 80 mV/s, potential range: +1.5 V to -1.5 V).

grain boundaries of the ITO. Concluding the above FESEM observation and the related EDS analyses, it obviously depicts that the oxides are virtually excluded in the spherical particles. Contrary to the results reported by Monk and Man [11], the reduction product of M_x ITO is absent in the present reduction spherical particle on ITO, which comprised exclusively In–Sn metallic solid solution.

Fig. 7 shows the VS response performed with as-received, 200 °C annealed ITO. It can be clearly seen that two definite features of all VS responses can be

observed in the negative potential region. A reduction current peak occurred in the potential more negative than -0.8 V. After the reduction current peak, the cathodic current increased with increasing the potential and held on linearly to the end of scanning; meanwhile, many bubbles, unlike spherical particles, can be visually observed on the ITO surface. Since the VS test was performed in aqueous 0.3 M HCl electrolyte, the bubbles can be reasonably regarded as hydrogen derived from the reduction of hydrogen ions on the cathodic surface.

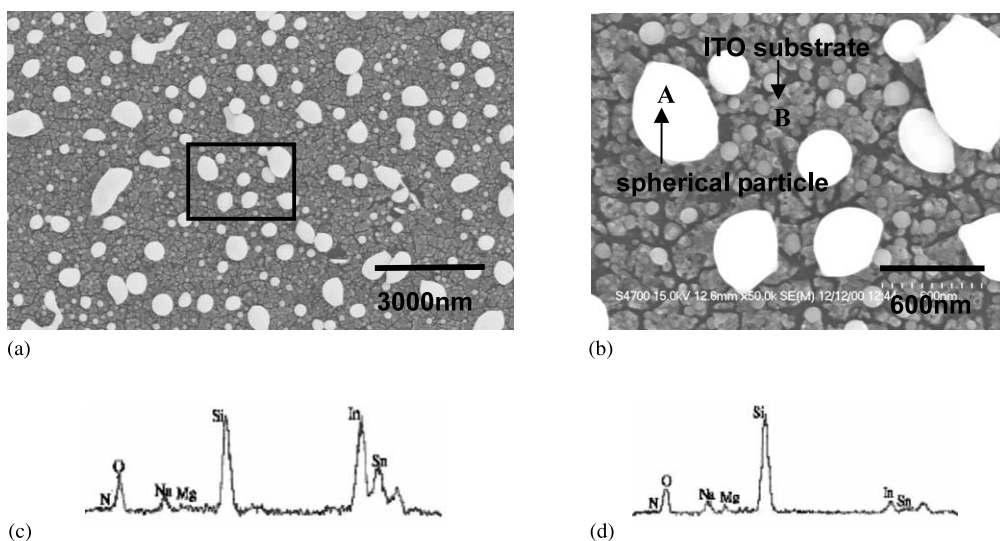


Fig. 5. (a) FESEM micrograph of as-received ITO after VS test; (b) magnified micrograph of the rectangular area in (a); (c) EDS analysis of the spherical particle (position A); and (d) EDS analysis of the ITO substrate (position B).

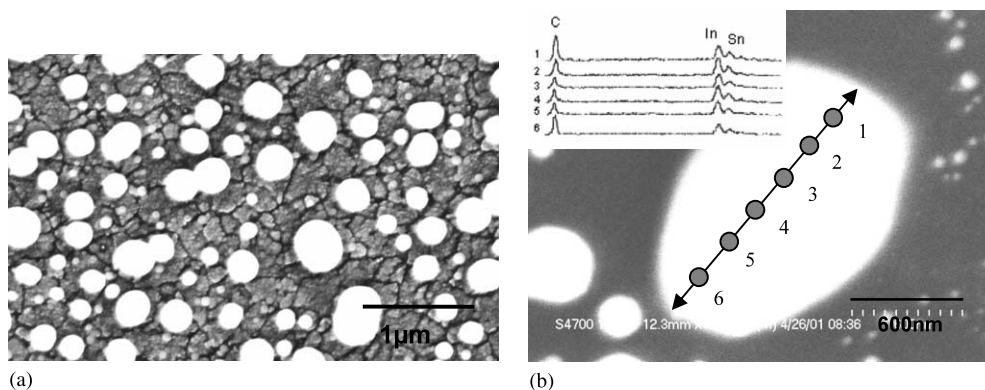


Fig. 6. (a) FESEM micrograph of ITO after applying constant potential at -1.5 V for 0.25 s. (b) FESEM micrograph of an isolated above-formed spherical particle and extracted with a carbon bond. EDS analyses of six local points within the isolated particle with 4 nm electron beam affixed.

The same result as that shown in Fig. 4, the reduction current peak occurred only in the first negative potential scanning and disappeared in succeeding scanning cycles. The reduction current peaks of the VS responses with as-received and 200°C annealed ITO were almost the same (Fig. 7(a)). Whereas, the reduction peak current of

the 500°C annealed ITO was significantly smaller than that of the other two specimens, ca. $17\text{--}40\text{ mA/cm}^2$. Moreover, the potential of the reduction current peak was shifted toward more negative value (Fig. 7(b)). These features implied that the surface of the ITO became relatively inactive after annealing at 500°C for 1

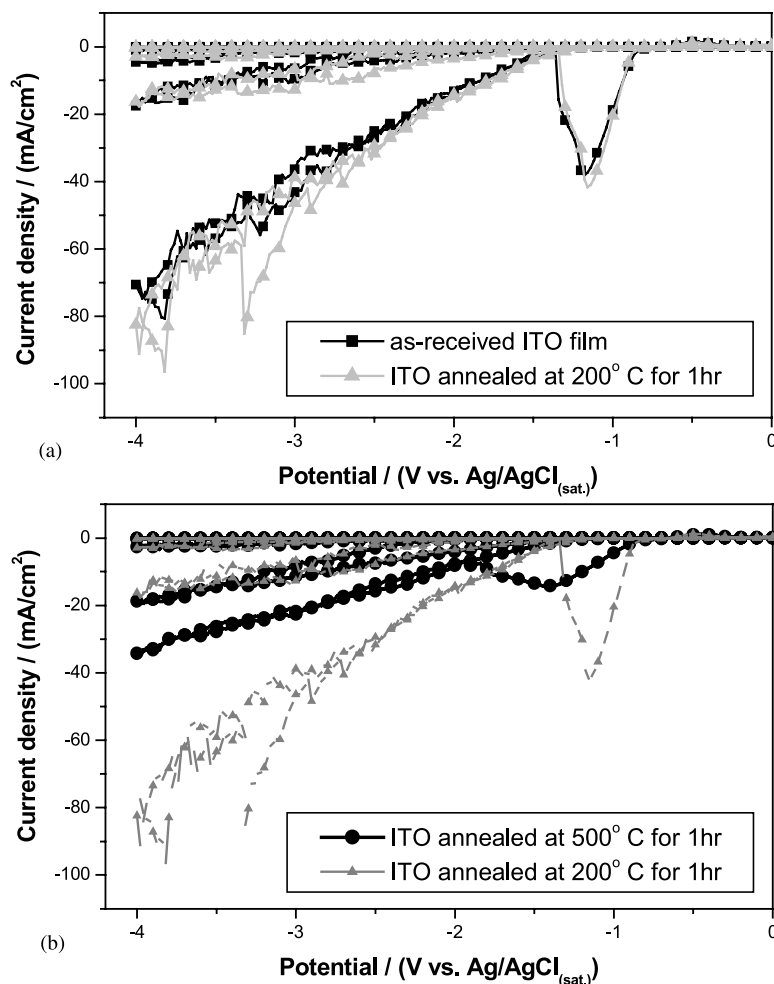


Fig. 7. The VS response of the ITO with different pretreatments: (a) as-received ITO and the ITO annealed at 200°C for 1 h, and (b) the ITO annealed at 500°C and 200°C for 1 h, respectively.

h. It probably means that the oxygen vacancies in ITO lattice are replenished with oxygen during annealing at 500 °C in the air, and the oxygen vacancy replenishment can decrease the carrier concentration and increase the resistivity of the ITO [15–18]. The result of VS also confirmed that the replenishment with oxygen was not sufficient to change the electrochemical behavior of ITO after annealing at 200 °C for 1 h.

From the result shown in Fig. 7, it can be clearly seen that the slope of the reduction current, which took place after the reduction current peak in more negative potential region, decreased progressively with increasing the scanning cycles. As shown in Fig. 7(a), the slope variation of the reduction current in the VS responses of both as-received and 200 °C annealed ITO films were almost the same in every scanning cycle; on the other hand, in the same scanning cycle the reduction current of 500 °C annealed ITO is obviously smaller than those of the other two specimens (see Fig. 7(b)). It implies that the 500 °C annealed ITO has less activity than that of the other two specimens for the reduction reaction of hydrogen ions.

3.3. Formation mechanism of the spherical reduction particles

In order to study the formation mechanism of the spherical particles, a scanning of potential ranging from 1.5 to –1.0 V was performed. This experiment enables the observation of the spherical particles just initiate on the ITO surface. The results of potential vs. current density and the corresponding FESEM micrograph of the ITO surface are presented in Fig. 8. It is interesting to note that some tiny spherical particles in a size of a few nanometers could be observed on the ITO surface and most of those particles were found merely around the grain boundaries. Meanwhile, slight dissolution of the grain boundaries also occurred. Therefore, it is evident that applying a cathodic current on the ITO in 0.3 M HCl would lead to dissolution of the grain boundaries of the ITO and then formation of the spherical reduction particles.

Based on the preceding results, the formation mechanism of the spherical particle could be postulated and illustrated in Fig. 9. As shown in Fig. 9(b), when the ITO electrode is cathodically polarized in 0.3 M HCl, both metallic ions (In^{3+} and Sn^{2+}) and oxygen ion O^{2-} would be first released from the ITO, especially from the grain boundaries of the ITO. The similar phenomenon was suggested by Baliga and Ghandhi [19] that the SnO_2 would probably be reduced to tin due to the nascent hydrogen generated at the surface of the tin-oxide surface by applying a cathodic current in various concentrations of HCl. Tousek [20] reported another reaction mechanism, where the metal oxide can be dissolved in the solution containing adsorbing anions,

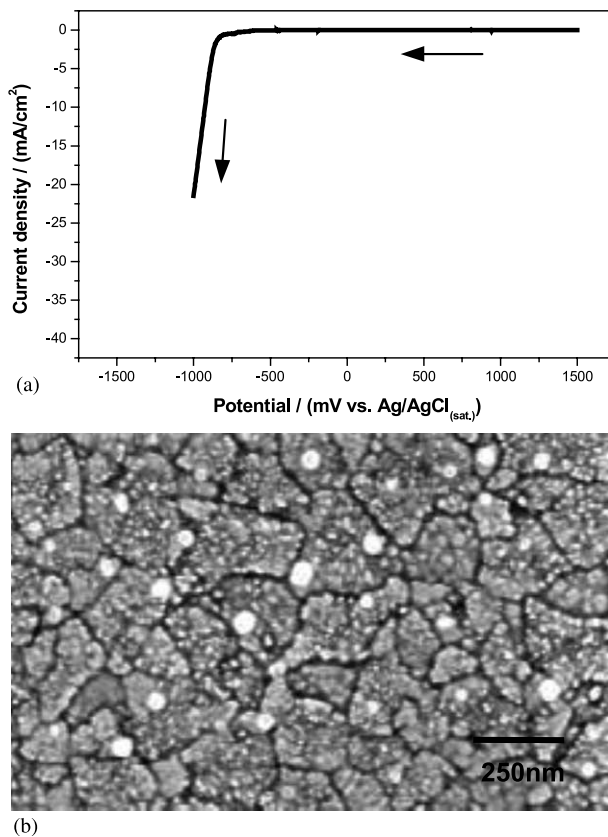


Fig. 8. (a) Scanning in a potential range from 1.5 to –1.0 V for the as-received ITO (scanning rate: 80 mV/s); (b) FESEM micrograph of the ITO surface after (a) scanning.

such as Cl^- in this study. It was significant to note that grain boundaries offered the preferential dissolution sites for releasing the above species, owing to their own high diffusion rate path and stored energy. When the grain boundaries are depleted, high concentration of metallic ions (In^{3+} and Sn^{2+}) could be accumulated in this depleted region. Subsequently, the metallic ions are reduced only on the ITO surface just adjacent to the depleted grain boundaries when the cathodic current is still applied (Fig. 9(b)). Moreover, the interfacial energy between the deposited In–Sn particles and 0.3 M HCl was so high that the particle inevitably assumed spherical shape to reduce the interfacial energy. Fig. 9(c) shows the presentation of the reduction reaction of hydrogen ions, which would achieve by applying cathodic charge and develop hydrogen bubbles on the ITO surface after the reduction of metallic ions in more negative potential region.

4. Conclusions

The electrochemical behavior for VS of the ITO electrode in 0.3 M HCl was studied in this work. A significant reduction current peak was observed during

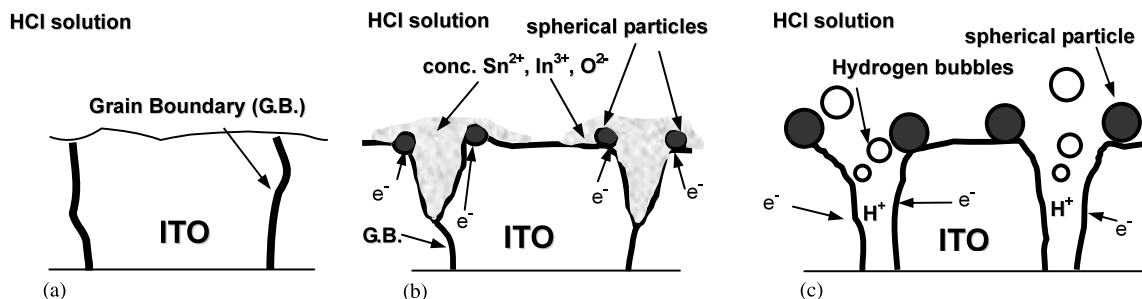


Fig. 9. Illustration of the sequential processes of the ITO under cathodic current applied (a) cross-sectional ITO; (b) dissolution of the grain boundaries of the ITO and formation of the spherical reduction particles under cathodic current applied and (c) evolution of hydrogen bubbles in more negative potential region.

the first negative potential scanning test. Numerous spherical In–Sn particles on the ITOs surface formed concurrently with occurrence of this reduction current peak. From FESEM observation and EDS analysis, it was found that formation of the reductive particles attended the depletion of grain boundaries. The annealing treatment of ITO at 500 °C for 1 h made ITO less active in its reduction reaction, possibly caused by the replenishment of current carrier oxygen-deficient site. Due to its high diffusion rate and stored energy, the grain boundary of the ITO is very sensitive to cathodic current applied, through which the grain boundary would dissolve preferentially. In the scanning period, after completion of the reduction current peak, reduction of hydrogen ions occurred in more negative potential region. Formation of the spherical reduction In–Sn particles was confirmed by FESEM observation and EDS analysis. A schematic diagram illustrating the processes related with formation of this In–Sn reduction particle was postulated.

Acknowledgements

The authors would like to acknowledge the valuable guidance from Dr. Y. Chang and Dr. J.H. Lee of RiTdisplay Corporation during the progress of the study.

References

- [1] R.H. Bube, A.L. Fahrenbruch, R. Sinclair, T.S. Anthony, C. Fortman, C.T. Lee, T. Thorpe, T. Yamashita, *IEEE Trans. Electron Devices* 31 (1989) 528.
- [2] V.P. Singh, D.C. Morton, M.R. Miller, *IEEE Trans. Electron Devices* 35 (1988) 38.
- [3] H. Kobayashi, T. Ishida, Y. Nakato, H. Tsubomura, *J. Appl. Phys.* 69 (1991) 1736.
- [4] C. Coutal, A. Azema, J.-C. Roustan, *Thin Solid Films* 288 (1996) 248.
- [5] O.P. Agnihotri, A.K. Sharma, B.K. Gupta, R. Thangaraj, *J. Phys. D* 11 (1978) 643.
- [6] K.L. Chopra, S. Major, D.K. Pandya, *Thin Solid Films* 102 (1983) 1–46.
- [7] J. Bruneaux, H. Cachet, M. Froment, J. Amblard, M. Mostafavi, *J. Electroanal. Chem.* 269 (1989) 375.
- [8] P.M.M.C. Bressers, E.A. Meulenkaamp, *J. Electrochem. Soc.* 145 (1998) 2225.
- [9] G. Folcher, H. Cachet, M. Froment, J. Bruneaux, *Thin Solid Films* 301 (1997) 242.
- [10] A.J. Bard, R. Parsons, J. Jordan (Eds.), *Standard Potentials in Aqueous Solutions*, IUPAC, Marcel Dekker, New York, 1985.
- [11] P.M.S. Monk, Che M. Man, *J. Mater. Sci.: Mater. Electron.* 10 (1999) 101.
- [12] Z. Wang, X. Hu, *Thin Solid Films* 392 (2001) 22.
- [13] Internal Report of RiTdisplay Corporation, 2001.
- [14] V. Vasu, A. Subrahmanyam, *Thin Solid Films* 193/194 (1990) 696.
- [15] D.V. Morgan, Y.H. Aliyu, R.W. Bunce, A. Salehi, *Thin Solid Films* 312 (1998) 268.
- [16] N.G. Patel, B.H. Lashkari, *J. Mater. Sci.* 27 (1992) 3026.
- [17] J.F. Smith, A.J. Aronson, D. Chen, W.H. Class, *Thin Solid Films* 72 (1980) 469.
- [18] V. Vasu, A. Subrahmanyam, *Thin Solid Films* 193/194 (1990) 696.
- [19] B.J. Baliga, S.K. Ghandhi, *J. Electrochem. Soc.* (1977) 1059.
- [20] J. Tousek, *Corros. Sci.* 15 (1975) 113.